European Cells and Materials Vol. 27 2014 (pages 26-38) DOI: 10.22203/eCM.v027a03 ISSN 1473-2262

REAL-TIME QUANTIFICATION OF MATRIX METALLOPROTEINASE AND INTEGRIN αvβ3 EXPRESSION DURING BIOMATERIAL-ASSOCIATED INFECTION IN A MURINE MODEL

Seyedmojtaba Daghighi[1], Jelmer Sjollema[1,*], Rene J.B. Dijkstra[1], Valery Jaspers[2], Sebastian A.J. Zaat[2], Henny C. van der Mei[1], and Henk J. Busscher[1]

[1]University of Groningen and University Medical Centre Groningen, Department of Biomedical Engineering, Groningen, The Netherlands

[2]Department of Medical Microbiology, CINIMA (Centre for Infection and Immunity Amsterdam), Academic Medical Centre, University of Amsterdam, Amsterdam, The Netherlands

Abstract

Biomaterial implants and devices increase the risk of microbial infections due to the biofilm mode of growth of infecting bacteria on implant materials, in which bacteria are protected against antibiotic treatment and the local immune system. Matrix-metalloproteinases (MMPs) and cell surface integrin receptors facilitate transmigration of inflammatory cells toward infected or inflamed tissue. This study investigates the relationship between MMP- and integrin-expression and the clearance of infecting *Staphylococcus aureus* around implanted biomaterials in a murine model. MMP- and integrin αvβ3-expression were monitored in mice, with and without subcutaneously implanted biomaterial samples, in the absence and presence of bioluminescent *S. aureus* Xen36. Staphylococcal persistence was imaged longitudinally over time using bioluminescence imaging. The activatable MMPSense®680 and integrin-targeted IntegriSense®750 probes were injected on different days after implantation and their signal intensity and localisation monitored using fluorescence imaging. After sacrifice 7 or 16 days post-implantation, staphylococci from biomaterial samples and surrounding tissues were cultured on agar-plates and presence of host inflammatory cells was histologically evaluated. MMP- and integrin-expression were equally enhanced in presence of staphylococci or biomaterials up to 7 days post-implantation, but their localisation along the biomaterial samples differed. Bacterial clearance from tissue was higher in the absence of biomaterials. It is of clinical relevance that MMP- and integrin-expression were enhanced in presence of both staphylococci and biomaterials, although the immune system in the presence of biomaterials remained hampered in eradicating bacteria during the first 7 days post-implantation.

Keywords: Immune response; bioluminescence; matrix metalloproteinase; fluorescence; integrin; infection; *Staphylococcus aureus*; implant.

*Address for correspondence:
Jelmer Sjollema
Department of Biomedical Engineering, W.J. Kolff Institute
University Medical Center Groningen
P.O. Box 196, 9700 AD Groningen, The Netherlands
Phone number: +31503633149
FAX Number: +31503633159
E-mail: j.sjollema@umcg.nl

Introduction

Biomaterials-Associated Infection (BAI) is a major complication in the use of biomaterial implants and devices for functional restoration. The onset of BAI is peri- or early post-operative bacterial contamination of the implant or surgical site, but bacteria can reach an implant site also after implantation through haematogenous spreading from infection elsewhere in the body (Busscher *et al.*, 2012). Once adhering, the organisms adapt a so-called "biofilm mode of growth", in which they embed themselves in a matrix of extracellular polymeric substances. In a biofilm, bacteria are protected against antibiotic treatment and the local immune system (Boelens *et al.*, 2000a; Flemming and Wingender, 2010). Consequently, BAI often results in surgical replacement of the implant or device, not seldom involving substantial morbidity, mortality and high costs to the healthcare system (Busscher *et al.*, 2012).

Implanted biomaterials provoke an inflammatory response, known as the Foreign Body Reaction (FBR). The onset of the FBR encompasses migration of neutrophils to the tissue adjacent to an implanted biomaterial (Anderson *et al.*, 2008). This acute phase resolves between a few hours to days and progresses to a type of inflammation characterised by chronic infiltration of mononuclear leukocytes, particularly monocyte-derived macrophages (Hu *et al.*, 2001; Luttikhuizen *et al.*, 2006). The inflammatory response is orchestrated in part by matrix metalloproteinases (MMPs) and integrins (Garcia, 2005; Jones *et al.*, 2008; MacLauchlan *et al*., 2009). In response to infectious stimuli, MMPs are expressed by activated leukocytes and are responsible for degradation of extracellular matrix components to facilitate migration of inflammatory cells, progression of inflammatory reactions and assisting in clearance of infection (Parks *et al.*, 2004). Integrins are transmembrane heterodimer receptors composed of α and β subunits, which mediate adhesion of leukocytes to the extracellular matrix (Hood and Cheresh, 2002). Integrin αvβ3, a receptor for a variety of extracellular matrix proteins containing arginine-glycine-aspartic acid (RGD) domains (Kerr, 1999; Hynes, 2002), facilitate cell migration, and mediate adhesion of monocytes and macrophages to adsorbed conditioning films on implanted biomaterial surfaces containing fibronectin (Kao *et al.*, 2001; Garcia, 2005; Keselowsky *et al.*, 2005) or vitronectin, collagen, fibrinogen and albumin (Wilson *et al.*, 2005; Anderson *et al.*, 2008), To summarise, biomaterial-adherent phagocytes express high levels of MMPs, and integrins in order to enable extracellular matrix remodelling and facilitate cell migration. These events lead to the release of cytokines and chemokines that can activate additional phagocytes. Therefore, these biomarkers play a pivotal role in the migration of leukocytes, and it is hypothesised that both biomarkers are increasingly expressed in the progression of bacterial clearance in a BAI.

Whereas a biomaterial implant or device may reduce the bactericidal activity of phagocytes (Zimmerli and Sendi, 2011), the host immune response may at the same time be activated by bacteria adhering to a biomaterial implant or present in surrounding tissue. In order to separate the role of infecting bacteria and the presence of a biomaterial implant or device in the immune response, we here apply bio-optical imaging in a murine model. Bio-optical imaging is increasingly used to monitor bacterial presence longitudinally in live animals (Daghighi *et al.*, 2012). Bio-optical imaging can either be performed in a bioluminescence or fluorescence mode (Hwang *et al.*, 2012; Ponomarev *et al.*, 2004). A number of bioluminescent bacterial strains are available for longitudinal monitoring of bacterial persistence. When growing on implanted biomaterials, their bioluminescence strongly correlated with *ex vivo* culturing of bacteria from explanted biomaterials after sacrifice (Kadurugamuwa *et al*., 2003; Engelsman *et al*., 2009). In addition, fluorescent marker molecules have been validated for use in *in vivo* imaging, like MMPSense®680 (Clapper *et al.*, 2011; Waschkau *et al.*, 2013) and IntegriSense®750 (Kossodo *et al.*, 2010; Snoeks *et al.*, 2010; Valdivia *et al.*, 2011), which are bio-activated by MMPs or targeted to integrin αvβ3, respectively.

The aim of this study is to assess the relationship between MMP- and integrin-expression and the clearance of infecting *Staphylococcus aureus*, one of the main causative organisms of BAI, in the presence and absence of an implanted biomaterial. To this end, Pebax® catheter sections (Wang *et al.*, 2004) were used as a model biomaterial and subcutaneously implanted in mice, after which mice were injected with bioluminescent *S. aureus* Xen36. Bio-activatable and targeted fluorescent imaging probes to quantify the expression of MMPs and integrin αvβ3 were injected 2, 5 and 11 days after implantation of the biomaterial samples. Bio-optical imaging in the bioluminescence mode allows for the longitudinal monitoring of the clearance of staphylococci, while measurements in the fluorescence mode including molecular tomography, enable localisation of MMPs and integrin αvβ3 around the biomaterial sample. Animals were sacrificed either 7 or 16 days after implantation for *ex vivo* microbiological and histological evaluations.

Materials and Methods

Bacterial strain

Experiments were conducted with bioluminescent *S. aureus* Xen36 (PerkinElmer, Waltham, MA, USA), derived from *S. aureus* ATCC49525, a virulent and biofilm forming clinical isolate from a patient with bacteraemia (Francis *et al.*, 2000) and used in earlier studies in murine models (Brand *et al.*, 2010; Pribaz *et al.,* 2011). Staphylococci were cultured from cryopreservative beads (Protect, Technical Surface Consultants, Heywood, UK) onto trypticase soy agar plates (TSA, Oxoid, Basingstoke, UK), containing 200 µg/mL kanamycin at 37 °C for 24 h in ambient air. Prior to each experiment, one highly bioluminescent colony was selected using an IVIS Imaging System (IVIS® Lumina II, Imaging System, PerkinElmer) to inoculate 5 mL of trypticase soy broth (TSB, Oxoid) at 37 °C for 24 h in ambient air. 100 µL of this culture was used to inoculate 10 mL of TSB and was grown for 16 h at 37 °C under continuous shaking at 120 rpm. Bacteria were harvested by centrifugation at 5000 g, for 5 min and washed twice with sterile 0.9 % NaCl, after which the bacterial pellet was suspended in the same solution and sonicated in an ice-water bath for 3 × 10 s at 30 W (Vibra cell model 375, Sonics and Materials, Newtown, CT, USA). Next, bacteria were resuspended in sterile 0.9 % NaCl to a final concentration of 10^9 bacteria per mL, as determined in a Bűrker-Tűrk counting chamber using phase contrast microscopy.

Fluorescent probes

MMPSense®680 (PerkinElmer) becomes fluorescent upon excitation around 680 nm with an emission wavelength of around 710 nm, after cleavage of its lysine-lysine bonds by active MMP-2, -3, -9 and -13 (Ntziachristos *et al.*, 2002; Jones *et al.*, 2012). IntegriSense®750 (PerkinElmer) is a targeted fluorescence imaging probe with an emission wavelength around 780 nm upon excitation with 750 nm wavelength light. The probe comprises a selective non-peptide small molecule integrin-antagonist that binds and accumulates at integrin αvβ3 receptors, predominantly marking the influx of immune cells, and remains localised for extended periods of time (Kossodo *et al.*, 2010). These fluorescent probes have successfully been applied to monitor MMPs or integrins in angiogenesis (Chen *et al.*, 2004), tumour microenvironment (Littlepage *et al.*, 2010), atherosclerosis (Deguchi *et al.*, 2006) and rheumatoid arthritis (Peterson *et al.*, 2010). They can be used simultaneously because of their distinct and non-overlapping excitation and emission wavelengths.

Animals and surgical procedure

Animal experiments and experimental protocols were approved (ID-5770) by the Ethics Committee for Animal Experiments of the University of Groningen, The Netherlands. Experiments were performed in female Balb/c OlaHsd immune-competent mice, aged 6-8 weeks with an averaged body weight of 23 ±3.2 g (Harlan Netherlands, Horst, The Netherlands). Groups of five mice were housed in separate, ventilated cages with free access to water. In order to prevent feed-associated auto-fluorescence, the mice received an alfalfa-free diet (Diet W, Abdiets, Woerden, The Netherlands) *ad libitum.*

Mice were randomly assigned to four groups (see Table 1). During surgery, mice were placed on a heating mat and anaesthesia was induced with 3.5 %, and maintained at 1.5 % isoflurane/O_2 (Zeneca, Zoetermeer, The Netherlands). The dorsal side of the mice were shaved in order to prevent bioluminescent light scattering and

Table 1. Number of animals involved in the *in vivo* experiments for each of the four experimental groups.

Experimental groups			Number of mice	
			Sacrificed at day 7	Sacrificed at day 16
1	No biomaterial sample	No bacteria	4	4
2	No biomaterial sample	Bacteria	7	4
3	Biomaterial sample	No bacteria	8	15
4	Biomaterial sample	Bacteria	8	15

Note that only 10 out of the 15 mice sacrificed at day 16 in groups 3 and 4 were subjected to microbiological and histological analysis.

the skin was disinfected with 70 % ethanol to reduce the surgical site infections. The ventral side of the mice were shaved as well in order to allow transmittance of the laser light during fluorescence molecular tomography (FMT). A 1 cm midline incision was made in the skin in the posterior cervical region and a subcutaneous pocket was created by blunt dissection. In the pockets of two groups of mice, sterile catheter sections, made of medical-grade polyether block amides (Pebax®, Raumedic®, Helmbrechts, Germany) were placed as biomaterial samples. Biomaterial samples cut out of the catheters were 1 cm in length and in order to avoid intraluminal bacterial colonisation, cut in half along their length. The biomaterial samples were aligned with the spine and the incisions were closed using a tissue adhesive (Dermabond, Ethicon, Somerville, NJ, USA). Two other groups of mice were subjected to surgery, but no biomaterial sample was inserted (sham-surgery). Buprenorfine (0.03 mg/kg) was administered subcutaneously once, as an analgesic directly after implantation.

Eight mice of the sham-surgery group received an injection of 10 µL sterile saline, while 11 mice were injected with an inoculum of 10^7 staphylococci in 10 µL saline. In the groups of mice that had received a biomaterial sample, twenty-three mice were injected with 10 µL sterile saline, and 23 mice received an inoculum with 10^7 bacteria in 10 µL saline alongside the biomaterial sample. In order to prevent bacterial leakage through the incision, bacterial injections were administered 48 h after implantation, i.e., after wound closure. Moreover, this time interval also allowed us to analyse the expression of MMPs and integrin αvβ3 in the context of the foreign body reaction before bacterial injection. The relatively high inoculum of 10^7 bacteria appeared the lowest inoculum size leading to both culture positive peri-implant tissue biopsies and biomaterial implants in earlier BAI murine models (Broekhuizen *et al.,* 2007).

For *in vivo* fluorescence imaging, mice under isoflurane/O_2 anaesthesia were injected with 2 nmol of each fluorescent probe in a volume of 150 µL for MMPSense®680 and 100 µL for IntegriSense®750 through retro-orbital vein injection at days 2, 5 and 11 days post-implantation.

Bio-optical imaging

In vivo bioluminescence imaging of bacterial presence

Bacterial clearance was evaluated using an *In Vivo* Imaging System (IVIS® Spectrum, PerkinElmer) on selected days over a period of 7 or 16 days. For imaging, mice were placed in the IVIS under 1.5 % isoflurane/O_2 anaesthesia, with their back exposed to the camera. After acquiring a grey-scale photograph, a bioluminescence image was obtained (exposure time 5 min) using a 21 x 21 cm field of view, binning of 4, 1/f aperture and open filters. Images were automatically corrected for background noise. Regions of Interest (ROIs) of 5 cm^2 were manually created for each mouse and imaging session. Total photon counts over the ROIs were converted to photon fluxes (p/s) due to bioluminescence using Living Image software (PerkinElmer).

In vivo fluorescence imaging of MMP- and integrin-expression

The fluorescence fluxes generated from the MMPs and integrin αvβ3 probes were quantified in the IVIS® system 24 h after their administration, i.e., at 3, 6 and 12 days post-implantation and in addition to the bioluminescence measurements. Images were acquired using epi-illumination, with excitation/emission at 675/710 nm for MMPSense®680, and 720/820 nm for IntegriSense®750. These filter combinations were chosen to avoid leakage of excitation light through the emission filter and optimise the ratio between fluorescence from the probe and auto-fluorescence from murine tissue. The emission spectrum of bacterial bioluminescence is located between 400 and 600 nm, with a maximum around 500 nm and is not interfering with the fluorescence spectra of the probes. Manually created ROIs were positioned to capture all the light from the entire spot created by fluorescence light, scattered by the skin. All ROIs were of equal size (7 cm^2) and shape for each mouse and imaging session.

Beam broadening due to scattering of fluorescent light is rigorously taken into account in a fluorescence molecular tomography system (FMT) to reveal the size and position of the fluorescence source (Ntziachristos *et al.,* 2002). Therefore, four randomly selected mice in each group of infected and non-infected mice with an implanted biomaterial sample were imaged using FMT (FMT 2500™, PerkinElmer), when under anaesthesia for the IVIS analysis (Kossodo *et al.*, 2010). Three-dimensional distributions of the probes around the implant site were obtained using dedicated FMT software with a resolution of 1 mm (i.e., voxel size is 1 mm^3) and calibrated against the fluorescence flux of a 0.4 µM solution of each of the probes in 100 µL demineralised water, according to the manufacturer's instructions. The 3D-images were acquired using trans-illumination with an excitation laser beam with a wavelength of 670 nm for MMPSense®680, and 745 nm for integriSense®750. Emission wavelengths were 690 and 780 nm respectively, as pre-configured by the manufacturer.

In order to determine to what extent MMP- and integrin-expression are co-localised and result from the presence of biomaterial samples, probe distributions around the biomaterial samples were analysed using autocorrelation functions. These autocorrelations were calculated for each mouse in a 2D-slice of the 3D-image, aligned along the coronal plane of the mouse at the position of the implant. Autocorrelations were calculated in the x-direction parallel to the length of the biomaterial sample and in the y-direction perpendicular to the sample length and over an angular width of ±10 degrees. In the x-direction, the autocorrelation was calculated using MATLAB routines (The MathWorks, Natick, MA, USA) according to:

$$autocorrelation(h) = \frac{\Sigma_{i=1}^{n(h)}\left(F(x_i) * F(x_i + h)\right)}{n(h)} \quad (1)$$

in which $F(x_i)$ is the fluorescence concentration at pixel location x_i and $n(h)$ is the number of pixels at a distance h. Autocorrelations in the y-direction were calculated by changing x into y. Autocorrelations presented were normalised with respect to the autocorrelation at a distance of 1 mm from the biomaterial sample.

Microbiological and histological *ex vivo* evaluations

After sacrifice at days 7 or 16 (see Table 1), an incision was made in the dorsal skin, the subcutaneous layer with adjacent skin was prepared free to make the biomaterial sample visible and a disk-shaped standardised biopsy of 12 mm in diameter, comprising the biomaterial sample with surrounding tissue, was taken. Biopsies were cut in halves, for quantitative microbiological culture and histological analysis, respectively. Five randomly chosen biopsies from each of the groups with implanted biomaterial samples taken 16 days after sacrifice were only visually inspected for the signs of infection and not further processed.

For microbiological culturing, a biomaterial sample was carefully separated from the surrounding tissue and both were separately placed in 1 mL of 0.9 % NaCl. Next, the biomaterial sample and tissues were sonicated for 5 s in 0.9 % NaCl (500 µL), after which the samples were 10-fold serially diluted and plated on blood agar plates. Agar plates were incubated for 24 h at 37 °C after which the numbers of colony forming units (CFUs) were counted.

For histological analysis, biopsy specimens were fixed in 10 % phosphate-buffered formaldehyde, embedded in plastic (methylmethacrylate/butylmethacrylate; Merck Schuchart, Hohenbrunn, Germany), and 3 µm sections were cut, deplastified, stained with haematoxylin-eosin and examined by light microscopy, or immuno-stained for MMP-2 and MMP-9 with anti- MMP2/MMP-9 antibodies (Millipore, Amsterdam, The Netherlands), and visualised with Vector Red and Vector Blue, respectively. Images of the immuno-stained sections were recorded with a Nuance multispectral imaging camera (PerkinElmer), allowing display of the antigens in pseudo colours (Van der Loos, 2010).

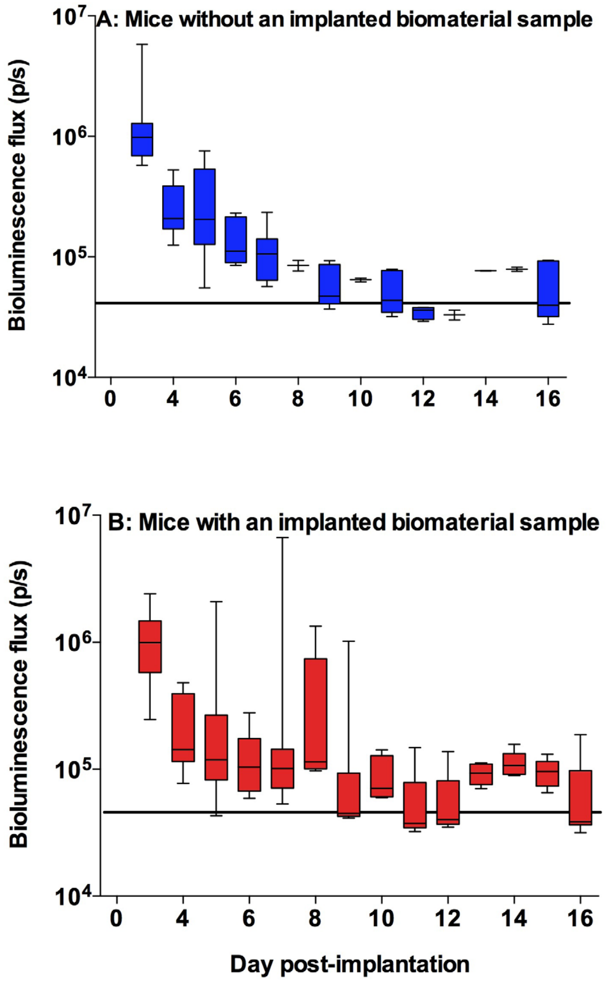

Fig. 1. Bioluminescence fluxes in mice without (**a**) and with (**b**) an implanted biomaterial sample arising from the presence of bioluminescent *S. aureus* Xen36 as a function of time post-implantation. Data are presented as medians with interquartile ranges. Note that up to day 7 data are from 23 mice, while after day 7 data represent values of the remaining 15 mice, since 8 mice of the groups were sacrificed at day 7 (see also Table 1). The horizontal lines represent the average bioluminescence fluxes from mice that were not inoculated with bacteria (i.e., only saline).

Statistical analysis

Data were analysed using SPSS 16 (SPSS, Chicago, IL, USA). Bioluminescence and fluorescence fluxes are represented as medians with interquartile ranges for each group of mice. *In vivo* bio-optical imaging and *ex vivo* culturing data were analysed using a Mann-Whitney test to assess significant differences between groups of mice. *P*-values < 0.05 were considered to indicate a statistically significant difference.

Results

***In vivo* bioluminescence imaging**

Bioluminescence fluxes from mice without and with implanted biomaterial samples are shown in Fig. 1. Initially, in the presence of staphylococci, the bioluminescence fluxes were equally high in groups of mice without (Fig.

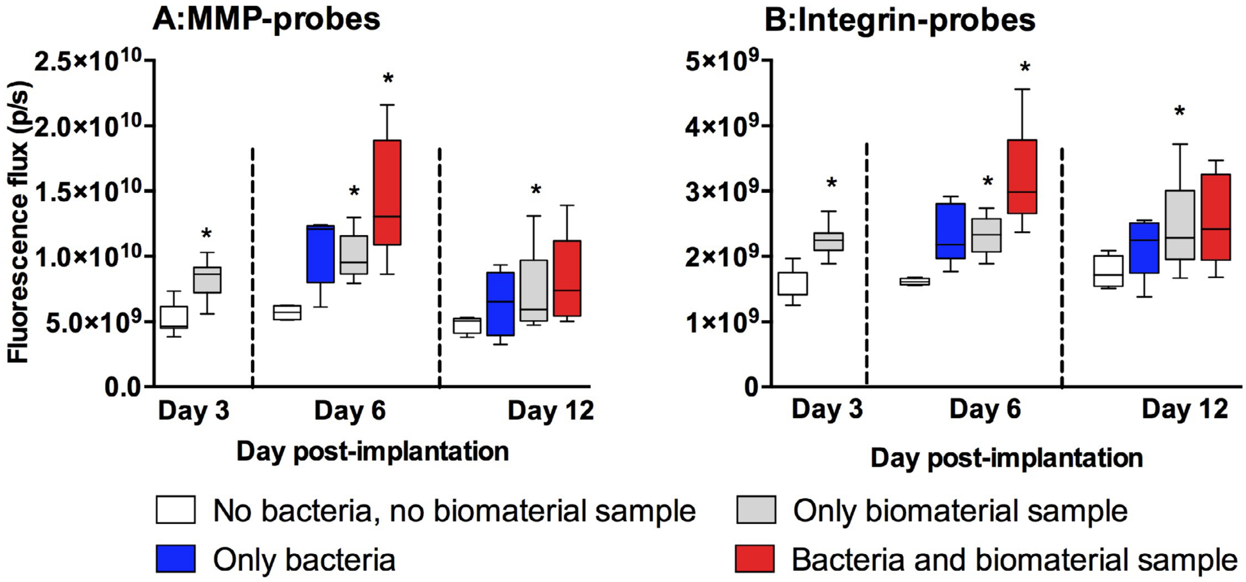

Fig. 2. Fluorescence fluxes generated by MMP activated (left) and integrin αvβ3 targeted (right) probes as a function of time post-implantation in the four different groups of mice (see Table 1). Probes were injected at 2, 5 and 11 days after implantation of the biomaterial samples and mice were imaged 24 h after injection. Data are presented as medians with interquartile ranges. Note that the different groups include different numbers of mice (for details see Table 1). (*) indicate significant differences as compared with the group of mice without an implanted biomaterial sample at the same day post-implantation.

1a) and with (Fig. 1b) biomaterial samples. Whereas the bioluminescence in the group of mice without a biomaterial sample steadily and consistently decreased over time in all mice, in the presence of a biomaterial sample strongly elevated levels of staphylococcal bioluminescence were observed in two mice, especially at days 7-9 post-implantation.

In vivo fluorescence imaging of MMPs and integrin αvβ3

Fig. 2 summarises the fluorescence fluxes in the different groups of mice at different time points post-implantation. These fluxes were much higher than the auto-fluorescence from biomaterial samples determined prior to fluorescence imaging. Three days post-implantation in absence of staphylococci, fluorescence was significantly higher in mice with an implanted biomaterial sample than in mice without an implanted biomaterial sample, and this difference continued to exist up to day 12. At day 6, staphylococcal presence increased the fluorescence fluxes from both probes significantly, both in the groups without and with implant. Twelve days post-implantation however, no significant differences related to the presence of bacteria were recorded, but the signal of the probes in the mice carrying an implant was still significantly ($p < 0.05$) higher than in mice without implant.

FMT images revealed that both probes distributed predominantly around the biomaterial samples (Fig. 3a). The concentrations of fluorophores showed high correlations over only 5 mm in the direction perpendicular to the length of a biomaterial sample for both MMP- and integrin probes, whereas correlations parallel to its length were high over 10 to 12 mm (Fig. 3b). Interestingly, the signals of the integrin probe showed higher correlations parallel to the length of a biomaterial sample than of MMP probes in all groups of mice, indicating that these probes did not fully co-localise, although co-localisation was stronger in the presence of staphylococci.

Ex vivo evaluation of biomaterial samples and surrounding tissues

Microbiological culturing

Seven days post-implantation, no significant differences in numbers of CFUs could be observed in tissue and biomaterial samples in both groups of bacterially challenged mice (Fig. 4). At 16 days post-implantation however, the number of CFUs were significantly lower in the mice without a biomaterial sample, whereas the number of CFUs in the mice with a biomaterial sample, both in the tissue and on the biomaterial sample, were not significantly lower. Visual inspections of randomly chosen biopsies revealed no clinical signs of infection, i.e., soft tissue swelling and pus formation.

Histological evaluation

Regardless of the presence of biomaterial samples, tissues of mice which had been inoculated with staphylococci and sacrificed at day 7 demonstrated strong inflammation with a dense infiltrate of phagocytic cells, predominantly neutrophils and macrophages (Fig. 5). The inflammatory reaction was milder at day 16 post-implantation than at day 7, with strongest inflammation in the mice with a biomaterial sample and bacteria. At 16 days, strong influx of cells expressing predominantly MMP-9, was observed adjacent to the biomaterial samples both in absence and presence of staphylococci (Fig. 6). In absence of implants the response was less intense.

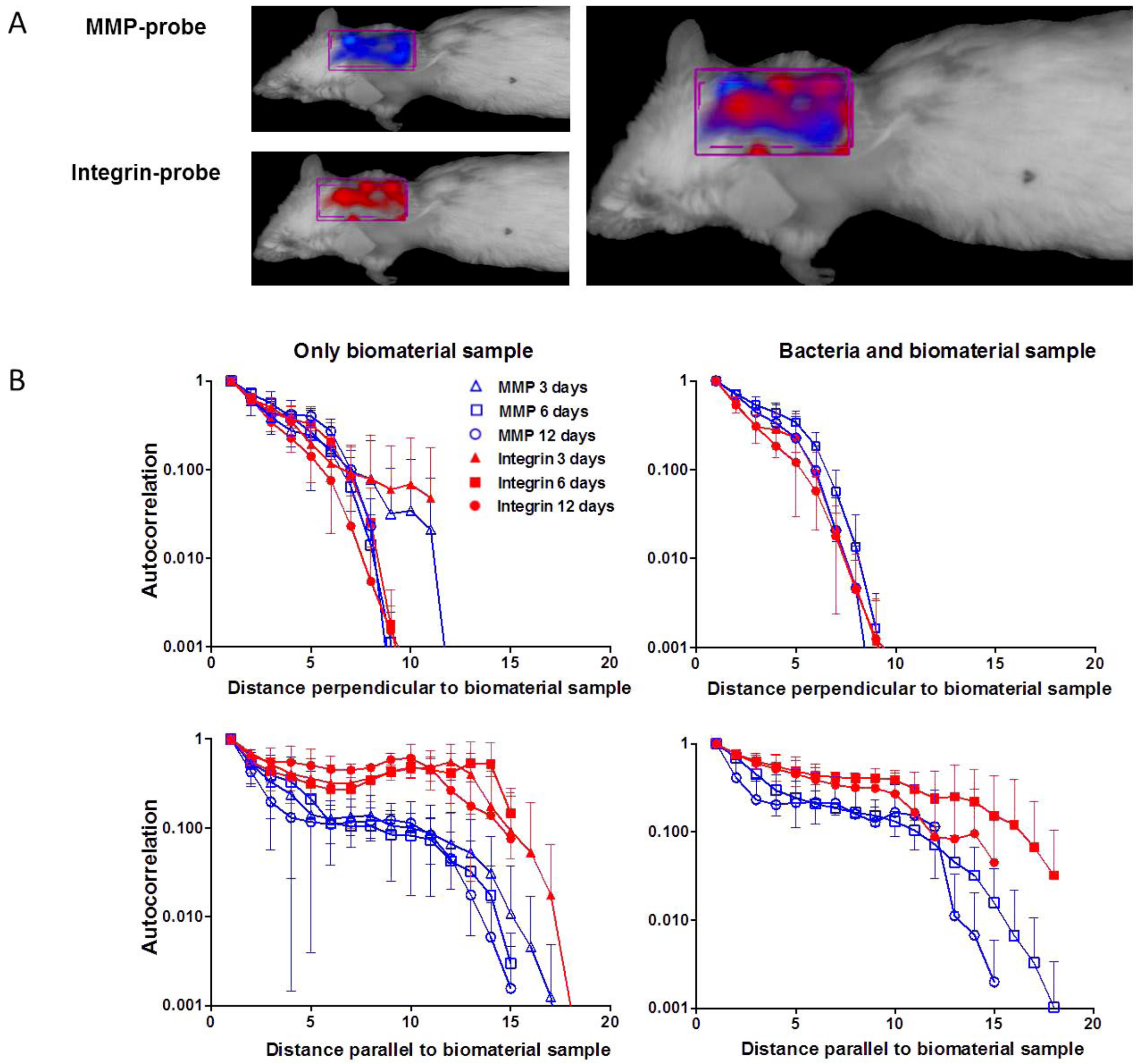

Fig. 3. Distribution of MMP activatable and integrin αvβ3 targeted probes in mice with an implanted biomaterial sample in absence and presence of a challenge with *S. aureus*, as obtained from 3D-fluorescence tomography (**a**). Autocorrelations of fluorescence distributions in mice that carry an implanted biomaterial sample in absence (left panel) or presence (right panel) of *S. aureus* Xen36 in the direction parallel and perpendicular to the length of a biomaterial sample at three time points after implantation. Error bars represent standard deviations of four mice in each group (**b**).

Discussion

We evaluated the simultaneous expression of MMPs and integrin αvβ3 around an implanted biomaterial in absence and presence of *S. aureus* using bio-optical imaging in a murine model. Through the combined use of *in vivo* bioluminescence and fluorescence imaging techniques, it was established that bacterial clearance was faster in absence than in presence of an implanted biomaterial (Fig. 4), despite enhanced expression of MMPs and integrin αvβ3 in the latter case (Fig. 2). Apparently, expression rates of MMPs and integrin αvβ3 do not correlate with the efficacy of the immune system to clear *S. aureus* in experimental murine biomaterial-associated infection.

MMPs are involved in multiple physiological and pathological processes such as infections, both in humans and in mice (Lopez-Otin *et al.*, 2009; Fanjul-Fernandez *et al.*, 2010). Expression of MMPs by neutrophils and monocytes can be induced by infecting bacteria (Wang *et al.*, 2005; Souza *et al.*, 2009). Staphylococci also produce MMP-like proteases (Gooz *et al.*, 2001; Medina *et al.*, 2005) themselves that activate the MMPSense®680 probe (see Fig. 7). However, we assume that the fluorescence flux from staphylococcal MMP-like proteases can be neglected relative to the fluorescence flux due to MMPs of neutrophils and monocytes, since after staphylococcal inoculation, differences between numbers of bacteria in mice with and without an implanted biomaterial sample were found to be non-significant at day 6 (see Figs. 1 and 4), whereas a clear enhancement in fluorescence flux from MMPSense®680 was observed in the presence of an implanted biomaterial sample. Moreover, integrin expression paralleled MMP expression.

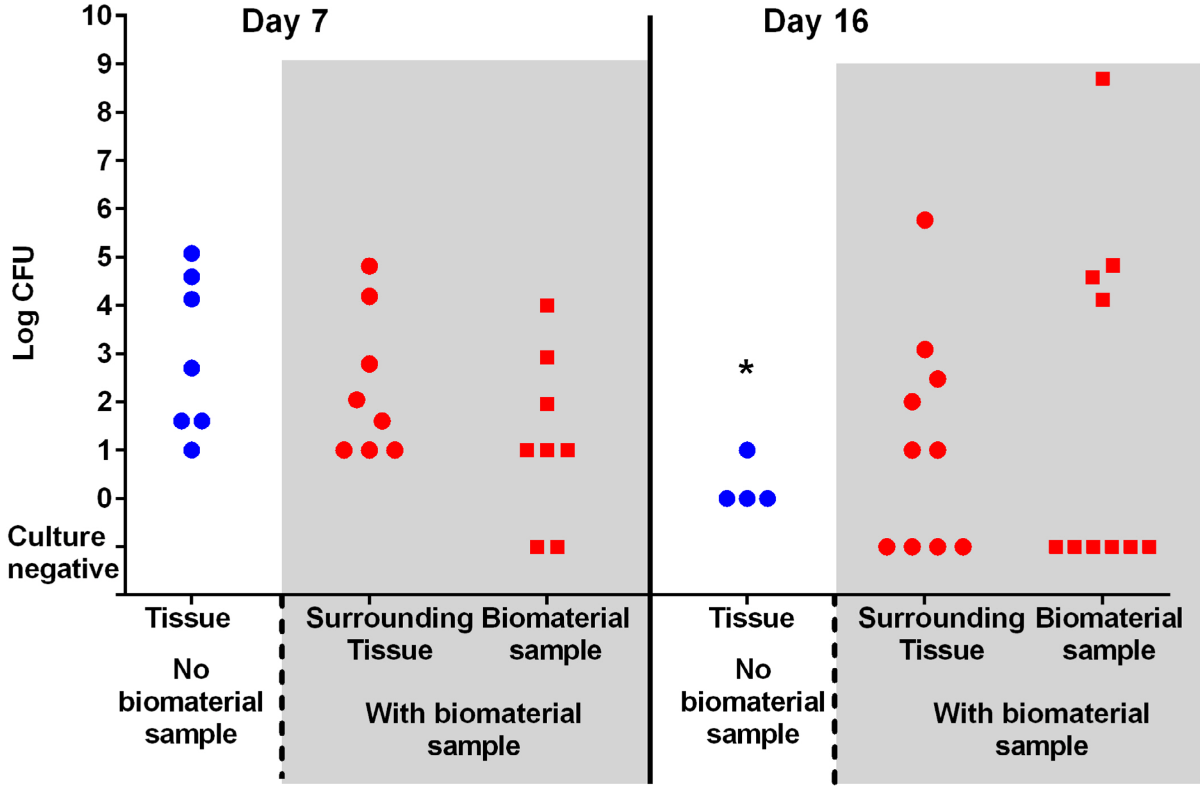

Fig. 4. Log CFUs of *S. aureus* Xen36 retrieved from tissues and biomaterial samples from mice without or with implanted biomaterial sample after sacrifice at day 7 and day 16. Note that all mice were challenged with staphylococci 48 h after surgery. Since no bacteria were injected in the control group, all cultures of this group were negative. The asterisk (*) indicates a significant decrease in number of CFUs as compared to the number of CFUs counted at day 7 in the same group of mice without a biomaterial sample.

Integrins have been studied both in humans and in animal models of inflammation (Damjanovich *et al.*, 1992; Singh *et al.*, 2000) but there is no *in vivo* information regarding the activation of integrins during BAI. *In vitro*, integrins serve as adhesion molecules to mediate cell adhesion to protein-coated biomaterials and to stimulate bacterial uptake into phagocytic cells. It has been suggested that integrin signalling at the transcriptional level regulates MMP expression (Fowler *et al.*, 2000). It may be hypothesised therefore, that MMPs and integrin activation are co-localised. The autocorrelation analysis (Fig. 3) demonstrates that the distribution of both biomarkers resembles the dimensions of the implanted biomaterial samples. However, the integrin signals aligned more strongly and over longer distances parallel to the length of the biomaterial samples than those of the MMPs. Integrins and MMPs thus were not fully co-localised, implying induction of expression of MMPs is not solely due to integrin signalling. The lack of co-localisation seems to disappear as soon as staphylococci are present. This may be due to the fact that staphylococci, when evenly distributed over the surface of the biomaterial sample, give rise to MMP activation in immune cells (Wang *et al.*, 2005; Souza *et al.*, 2009), in addition to the activation caused by the biomaterial itself. No differences were found in the distributions of biomarkers perpendicular to the lengths of the biomaterial samples, although integrins are cell wall associated while MMPs are excreted.

As a major advantage of bio-optical imaging, bacterial persistence around an implanted biomaterial and the associating FBR can be monitored in a quantitative way in one and the same animal, strongly reducing the numbers of animals needed. At day 16, the bioluminescence of the mice correlated with results from microbiological culturing and the decrease in fluorescence fluxes due to activation both MMP and integrin probes correlated with the decrease in the density of inflammatory cells from day 7 to day 16 in histologically examined specimens.

In conclusion, through the combined use of bioluminescent and fluorescent *in vivo* imaging techniques, it has been demonstrated for the first time that MMP and integrin expression are simultaneously enhanced in the presence of staphylococci or biomaterials for up to 6 days post-implantation in mice. Activation was strongest in the presence of staphylococci together with an implanted biomaterial, which confirms our hypothesis. In accordance with the notion that biomaterials increase the susceptibility to infection, bacterial clearance was higher in the absence than in the presence of implanted biomaterials, indicating that expression of MMPs and integrin was not correlated with an effective immune response and bacterial clearance in BAI. As a protracted and high level pro-inflammatory response may be associated with increased susceptibility to infection (Boelens *et al.*, 2000b), the up-regulated expression of MMPs and integrin may in fact be indicators of an exaggerated inflammatory response, which may

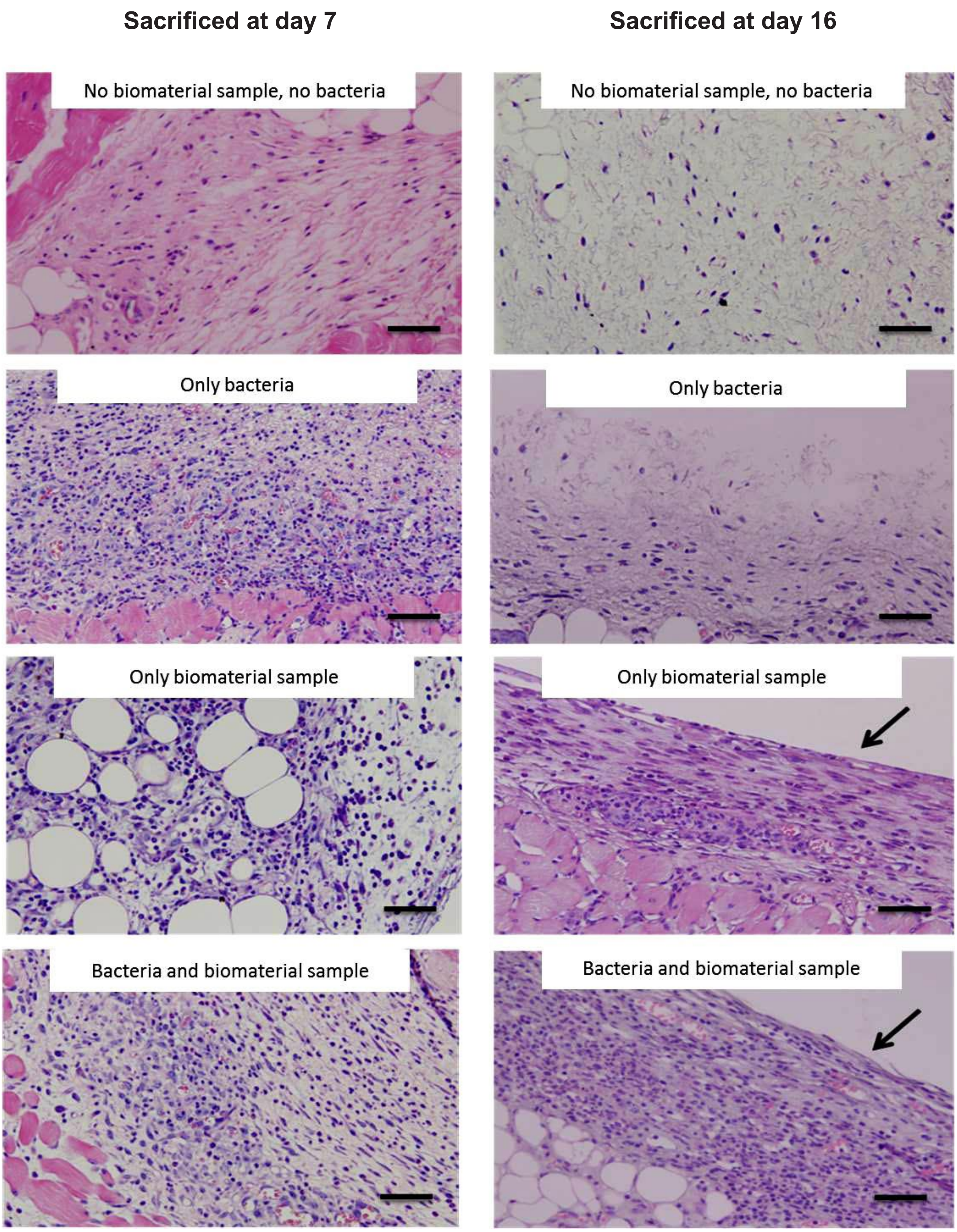

Fig. 5. Haematoxylin-eosin stained sections of biopsies retrieved from mice subjected to sham surgery or with implanted biomaterial samples, injected with saline or with *S. aureus* Xen36, 48 h after surgery, after 7 (left panel) and 16 (right panel) days post-surgery. Seven days post-surgery, a high density of purple-stained neutrophils and macrophages can be seen in all groups, except in the group with no implanted biomaterial sample and in absence of staphylococci. In comparison, 16 days after sacrifice, biopsies in all groups showed a less intense inflammatory response. Bars indicate 50 µm; arrows indicate the location of the interface with the biomaterial sample.

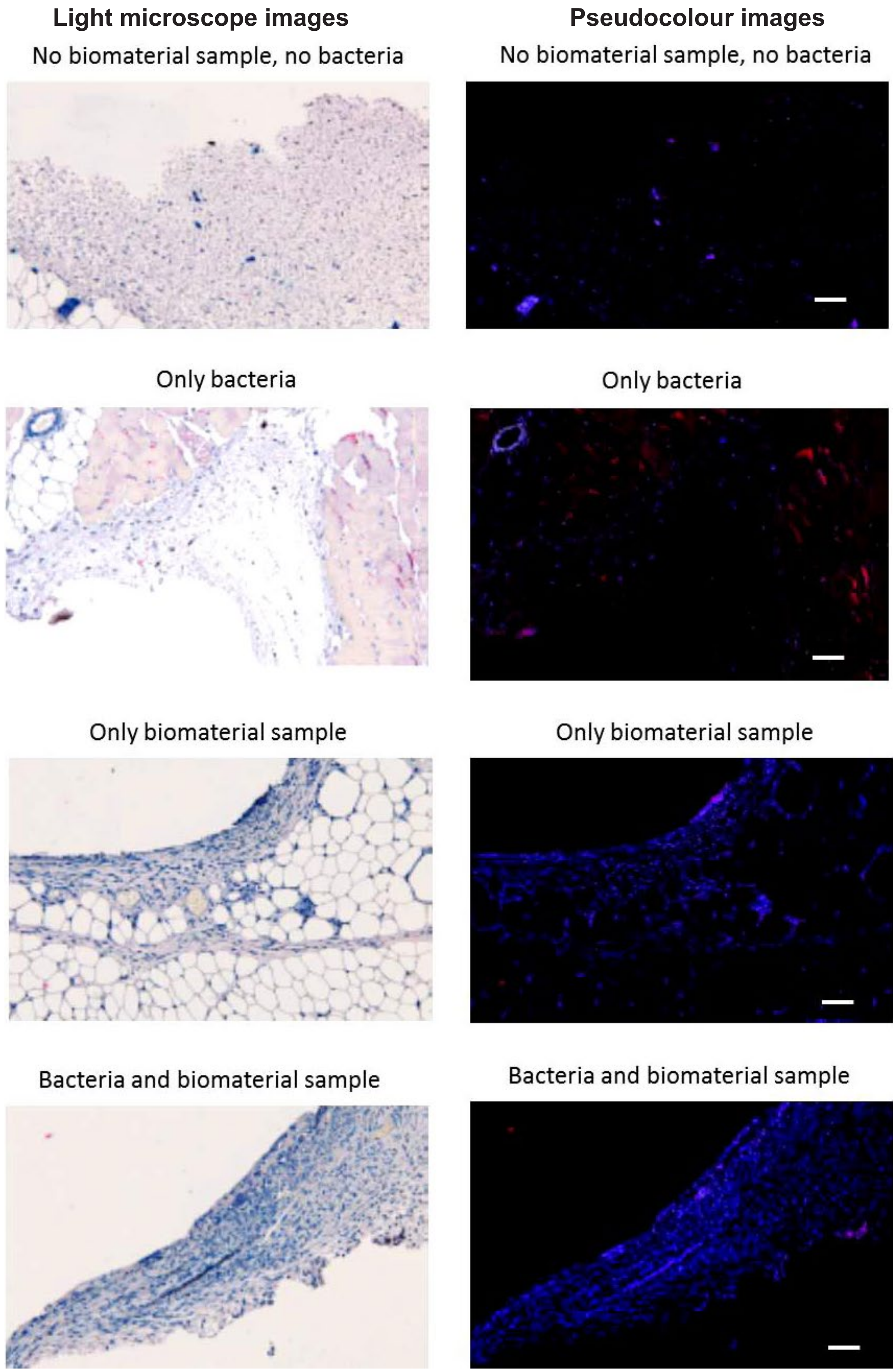

Fig. 6. MMP-2 and MMP-9 expression in tissue of mice in absence and presence of *S. aureus* for the sham-surgery group (without an implanted biomaterial sample), and the group of mice with implanted biomaterial samples after sacrifice at day 16. Sections were stained for MMP-2 (red) and MMP-9 (blue). The left panels are light microscopic images and the right panels are pseudo-colour images of corresponding sections. MMP-2 expression was seen in muscle fibres (e.g., in sham-surgery group with bacteria). Bars represent 20 µm.

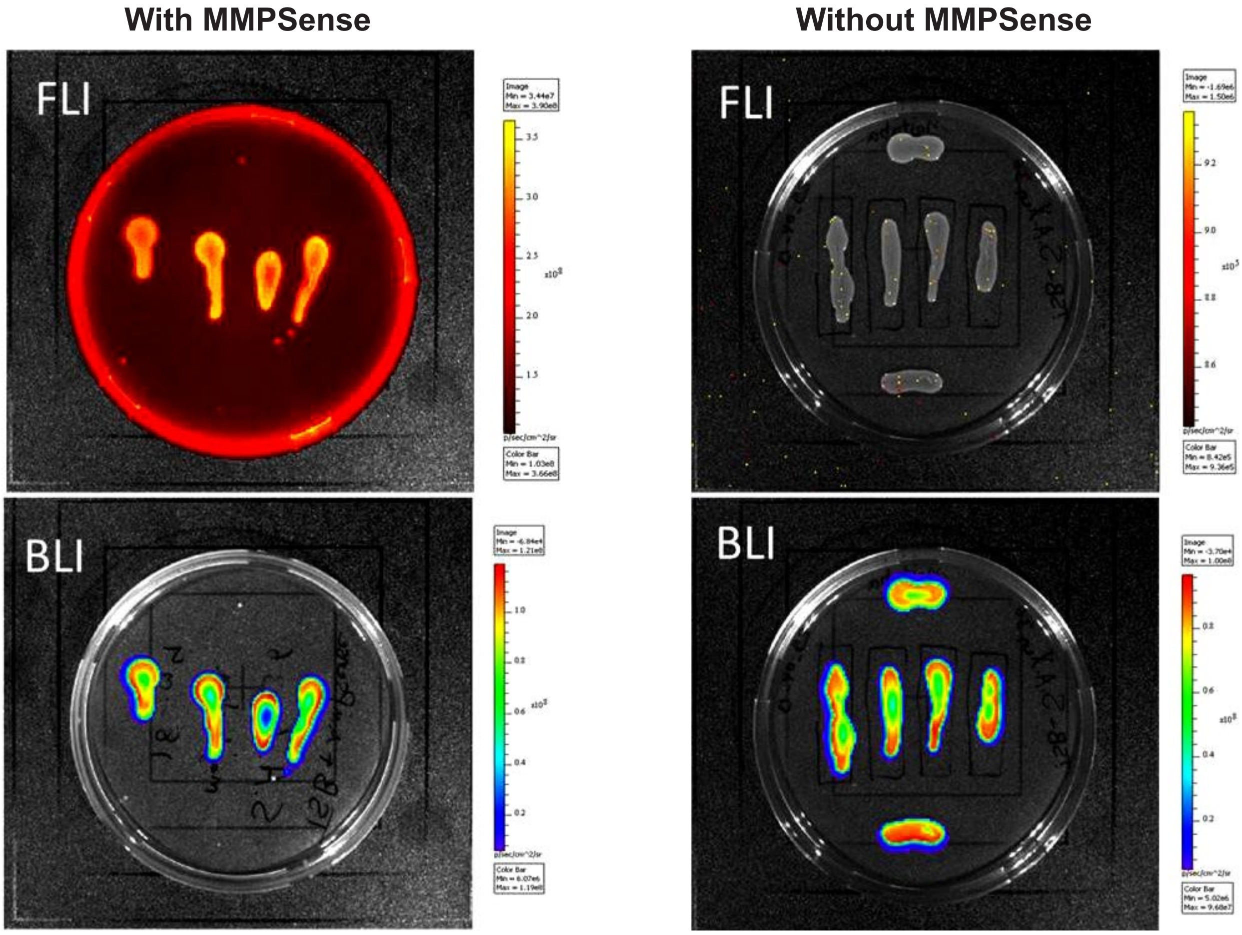

Fig. 7. Fluorescence (FLI) and bioluminescence images (BLI) of bioluminescent *S. aureus* Xen36 colonies grown on TSA with or without 2 nmol MMPSense®680 added per plate, taken in order to evaluate whether bacterial proteases are able to activate the MMPSense®680probe. From a comparison of the bioluminescence and fluorescence images, it can be concluded that *S. aureus* Xen36 is able to activate MMPsense®680. The low fluorescence measured on the agar with MMPsense is due to weak fluorescence of the non-activated probe.

be the cause of increased susceptibility to infection in patients carrying a biomaterial implant or device, rather than a sign of an effective immune response. The enhanced fluorescence from fluorescent probes early after BAI may help in distinguishing inflammation due to a sterile implant and BAI itself. Further studies may pave the way for clinical application of fluorescence imaging in image-guided implant debridement and support decision-making regarding antibiotic treatment of BAI or immediate implant replacement.

Acknowledgments

The authors would like to thank Martijn Riool and Leonie de Boer for histological evaluations and Peter Plomp for assistance in animal experiments. This research forms part of the Project P4.01 NANTICO of the research program of the BioMedical Materials institute, co-funded by the Dutch Ministry of Economic Affairs.

References

Anderson JM, Rodriguez A, Chang DT (2008) Foreign body reaction to biomaterials. Semin Immunol **20**: 86-100.

Boelens JJ, Dankert J, Murk JL, Weening JJ, van der Poll T, Dingemans KP, Koole L, Laman JD, Zaat SA (2000a) Biomaterial-associated persistence of *Staphylococcus epidermidis* in pericatheter macrophages. J Infect Dis **181**: 1337-1349.

Boelens JJ, van der Poll T, Zaat SA, Murk JL, Weening JJ, Dankert J (2000b) Interleukin-1 receptor type I gene-deficient mice are less susceptible to *Staphylococcus epidermidis* biomaterial-associated infection than are wild-type mice. Infect Immun **68**: 6924-6931.

Brand AM, de Kwaadsteniet M, Dicks LM (2010) The ability of nisin F to control *Staphylococcus aureus* infection in the peritoneal cavity, as studied in mice. Lett Appl Microbiol **51**: 645-649.

Broekhuizen CAN, De Boer L, Schipper K, Jones CD, Quadir S, Feldman RG, Dankert J, Vandenbroucke-Grauls CM, Weening JJ, Zaat SA (2007) Peri-implant tissue is an important niche for *Staphylococcus epidermidis* in experimental biomaterial-associated infection in mice. Infect Immun **75:**1129-1136.

Busscher HJ, Van der Mei HC, Subbiahdoss G, Jutte PC, Van den Dungen JJ, Zaat SA, Schultz MJ, Grainger DW (2012) Biomaterial-associated infection: locating the finish line in the race for the surface. Sci Transl Med **4**: 153rv110.

Chen X, Conti PS, Moats RA (2004) *In vivo* near-infrared fluorescence imaging of integrin alphavbeta3 in brain tumor xenografts. Cancer Res **64**: 8009-8014.

Clapper ML, Hensley HH, Chang WC, Devarajan K, Nguyen MT, Cooper HS (2011) Detection of colorectal adenomas using a bioactivatable probe specific for matrix metalloproteinase activity. Neoplasia **13**: 685-691.

Daghighi S, Sjollema J, Jaspers V, De Boer L, Zaat SA, Dijkstra RJ, Van Dam GM, Van der Mei HC, Busscher HJ (2012) Persistence of a bioluminescent *Staphylococcus aureus* strain on and around degradable and non-degradable surgical meshes in a murine model. Acta Biomater **8**: 3991-3996.

Damjanovich L, Albelda SM, Mette SA, Buck CA (1992) Distribution of integrin cell adhesion receptors in normal and malignant lung tissue. Am J Respir Cell Mol Biol **6**: 197-206.

Deguchi JO, Aikawa M, Tung CH, Aikawa E, Kim DE, Ntziachristos V, Weissleder R, Libby P (2006) Inflammation in atherosclerosis: visualizing matrix metalloproteinase action in macrophages *in vivo*. Circulation **114**: 55-62.

Engelsman AF, Van der Mei HC, Francis KP, Busscher HJ, Ploeg RJ, Van Dam GM (2009) Real time noninvasive monitoring of contaminating bacteria in a soft tissue implant infection model. J Biomed Mater Res Part B: Appl Biomater **88B**:123-129.

Fanjul-Fernandez M, Folgueras AR, Cabrera S, Lopez-Otin C (2010) Matrix metalloproteinases: evolution, gene regulation and functional analysis in mouse models. Biochim Biophys Acta **1803**: 3-19.

Flemming HC, Wingender J (2010) The biofilm matrix. Nat Rev Microbiol **8**: 623-633.

Fowler T, Wann ER, Joh D, Johansson S, Foster TJ, Hook M (2000) Cellular invasion by *Staphylococcus aureus* involves a fibronectin bridge between the bacterial fibronectin-binding MSCRAMMs and host cell beta1 integrins. Eur J Cell Biol **79**: 672-679.

Francis KP, Joh D, Bellinger-Kawahara C, Hawkinson MJ, Purchio TF, Contag PR (2000) Monitoring bioluminescent *Staphylococcus aureus* infections in living mice using a novel luxABCDE construct. Infect Immun **68**: 3594-3600.

Garcia AJ (2005) Get a grip: integrins in cell-biomaterial interactions. Biomaterials **26**: 7525-7529.

Gooz M, Gooz P, Smolka AJ (2001) Epithelial and bacterial metalloproteinases and their inhibitors in *H. pylori* infection of human gastric cells. Am J Physiol Gastrointest Liver Physiol **281**: G823-832.

Hood JD, Cheresh DA (2002) Role of integrins in cell invasion and migration. Nat Rev Cancer **2**: 91-100.

Hu WJ, Eaton JW, Ugarova TP, Tang L (2001) Molecular basis of biomaterial-mediated foreign body reactions. Blood **98**: 1231-1238.

Hwang JY, Wachsmann-Hogiu S, Ramanujan VK, Ljubimova J, Gross Z, Gray HB, Medina-Kauwe LK, Farkas DL (2012) A multimode optical imaging system for preclinical applications *in vivo*: technology development, multiscale imaging, and chemotherapy assessment. Mol Imaging Biol **14**: 431-442.

Hynes RO (2002) Integrins: bidirectional, allosteric signaling machines. Cell **110**: 673-687.

Jones EF, Schooler J, Miller DC, Drake CR, Wahnishe H, Siddiqui S, Li X, Majumdar S (2012) Characterization of human osteoarthritic cartilage using optical and magnetic resonance imaging. Mol Imaging Biol **14**: 32-39.

Jones JA, McNally AK, Chang DT, Qin LA, Meyerson H, Colton E, Kwon IL, Matsuda T, Anderson JM (2008) Matrix metalloproteinases and their inhibitors in the foreign body reaction on biomaterials. J Biomed Mater Res A **84**: 158-166.

Kadurugamuwa JL, Sin L, Albert E, Yu J, Francis K, De Boer M, Rubin M, Bellinger-Kawahara C, Parr Jr T, Contag PR (2003) Direct continuous method for monitoring biofilm infection in a mouse model. Infect Immun **71**: 882-890.

Kao WJ, Lee D, Schense JC, Hubbell JA (2001) Fibronectin modulates macrophage adhesion and FBGC formation: the role of RGD, PHSRN, and PRRARV domains. J Biomed Mater Res **55**: 79-88.

Kerr JR (1999) Cell adhesion molecules in the pathogenesis of and host defence against microbial infection. Mol Pathol **52**: 220-230.

Keselowsky BG, Collard DM, Garcia AJ (2005) Integrin binding specificity regulates biomaterial surface chemistry effects on cell differentiation. Proc Natl Acad Sci USA **102**: 5953e7.

Kossodo S, Pickarski M, Lin SA, Gleason A, Gaspar R, Buono C, Ho G, Blusztajn A, Cuneo G, Zhang J, Jensen J, Hargreaves R, Coleman P, Hartman G, Rajopadhye M, Duong le T, Sur C, Yared W, Peterson J, Bednar B (2010) Dual *in vivo* quantification of integrin-targeted and protease-activated agents in cancer using fluorescence molecular tomography (FMT). Mol Imaging Biol **12**: 488-499.

Littlepage LE, Sternlicht MD, Rougier N, Phillips J, Gallo E, Yu Y, Williams K, Brenot A, Gordon JI, Werb Z (2010) Matrix metalloproteinases contribute distinct roles in neuroendocrine prostate carcinogenesis, metastasis, and angiogenesis progression. Cancer Res **70**: 2224-2234.

Lopez-Otin C, Palavalli LH, Samuels Y (2009) Protective roles of matrix metalloproteinases: from mouse models to human cancer. Cell Cycle **8**: 3657-3662.

Luttikhuizen DT, Harmsen MC, Van Luyn MJ (2006) Cellular and molecular dynamics in the foreign body reaction. Tissue Eng **12**: 1955-1970.

MacLauchlan S, Skokos EA, Meznarich N, Zhu DH, Raoof S, Shipley JM, Bornstein P, Kyriakides TR (2009) Macrophage fusion, giant cell formation, and the foreign body response require matrix metalloproteinase 9. J Leukoc Biol **85**: 617e26

Medina C, Santana A, Llopis M, Paz-Cabrera MC, Antolin M, Mourelle M, Guarner F, Vilaseca J, Gonzalez C, Salas A, Quintero E, Malagelada JR (2005) Induction of colonic transmural inflammation by *Bacteroides fragilis*: implication of matrix metalloproteinases. Inflamm Bowel Dis **11**: 99-105.

Ntziachristos V, Tung CH, Bremer C, Weissleder R (2002) Fluorescence molecular tomography resolves protease activity *in vivo*. Nat Med **8**: 757-760.

Parks WC, Wilson CL, Lopez-Boado YS (2004) Matrix metalloproteinases as modulators of inflammation and innate immunity. Nat Rev Immunol **4**: 617-629.

Peterson JD, Labranche TP, Vasquez KO, Kossodo S, Melton M, Rader R, Listello JT, Abrams MA, Misko TP (2010) Optical tomographic imaging discriminates between disease-modifying anti-rheumatic drug (DMARD) and non-DMARD efficacy in collagen antibody-induced arthritis. Arthritis Res Ther **12**: R105.

Ponomarev V, Doubrovin M, Serganova I, Vider J, Shavrin A, Beresten T, Ivanova A, Ageyeva L, Tourkova V, Balatoni J, Bornmann W, Blasberg R, Gelovani Tjuvajev J (2004) A novel triple-modality reporter gene for whole-body fluorescent, bioluminescent, and nuclear noninvasive imaging. Eur J Nucl Med Mol Imaging **31**: 740-751.

Pribaz, JR, Bernthal NM, Billi F, Cho JS, Ramos RI, Guo Y, Cheung AL, Francis KP, Miller LS (2011) Mouse model of chronic post-arthroplasty infection: Noninvasive *in vivo* bioluminescence imaging to monitor bacterial burden for long-term study. J Orthop Res **29**: 1621-1626.

Singh B, Fu C, Bhattacharya J (2000) Vascular expression of the alpha(v)beta(3)-integrin in lung and other organs. Am J Physiol Lung Cell Mol Physiol **278**: L217-226.

Snoeks TJ, Lowik CW, Kaijzel EL (2010) '*In vivo*' optical approaches to angiogenesis imaging. Angiogenesis **13**: 135-147.

Souza LF, Jardim FR, Sauter IP, Souza MM, Barreto F, Margis R, Bernard EA (2009) Lipoteichoic acid from *Staphylococcus aureus* increases matrix metalloproteinase 9 expression in RAW 264.7 macrophages: modulation by A2A and A2B adenosine receptors. Mol Immunol **46**: 937-942.

Valdivia YAM, Wong K, He TC, Xue Z, Wong ST (2011) Image-guided fiberoptic molecular imaging in a VX2 rabbit lung tumor model. J Vasc Interv Radiol **22**: 1758-1764.

Van der Loos CM (2010) Chromogens in multiple immunohistochemical staining used for visual assessment and spectral imaging: The colorful future. J Histotechnol **33**: 31-40.

Wang Q, Brunner HR, Burnier M (2004) Determination of cardiac contractility in awake unsedated mice with a fluid-filled catheter. Am J Physiol Heart Circ Physiol **286**: H806-814.

Wang YY, Myhre AE, Pettersen SJ, Dahle MK, Foster SJ, Thiemermann C, Bjornland K, Aasen AO, Wang JE (2005) Peptidoglycan of *Staphylococcus aureus* induces enhanced levels of matrix metalloproteinase-9 in human blood originating from neutrophils. Shock **24**: 214-218.

Waschkau B, Faust A, Schafers M, Bremer C (2013) Performance of a new fluorescence-labeled MMP inhibitor to image tumor MMP activity *in vivo* in comparison to an MMP-activatable probe. Contrast Media Mol Imaging **8**: 1-11.

Wilson CJ, Clegg RE, Leavesley DI, Pearcy MJ (2005) Mediation of biomaterial-cell interactions by adsorbed proteins: A review. Tissue Eng **11:** 1-18.

Zimmerli W, Sendi P (2011) Pathogenesis of implant-associated infection: the role of the host. Semin Immunopathol **33**: 295-306.

Discussion with Reviewers

R. Luginbuehl: Please elucidate on the selected animal model, i.e., why is a subcutaneous model chosen in conjunction with catheters that are implanted typical in spaces with "high liquid flows". In addition subcutaneous spaces are typically lower in oxygen concentration and thus, I am wondering what the effect on the selected strains is as they are cultivated at norm Ox levels?

Authors: We agree with the reviewer that catheters are normally placed in spaces with liquid flows. The Pebax® catheter was used as a model biomaterial and not used as a catheter. Moreover, we did not want to study catheter-related infection, in which case indeed we would have chosen another implantation site. Accordingly, we did not verify the effect of varying Ox-levels.

R. Luginbuehl: Why was this specific animal model selected? Since catheter-related infections are not the objective of the research study, the selected model device has to be even more questioned as the tube offers a good protection for the bacteria. One of the findings was that "bacterial clearance from tissue was higher in absence of biomaterials" – which I consider is obvious as the bacterial proliferation is fundamentally different. The tube is an incubator for bacteria well protected from the immune system and clearance and a steady source of new bacteria. In my opinion a non-hollow implant would have done a better job.

Authors: The reviewer is entirely right, which is exactly the reason why we cut the catheter sections in half along their length.

D. Grainger: This statement is intriguing: "differences between numbers of bacteria in mice with and without a catheter section were found to be non-significant at day 6 (see Figs. 1 and 4)…". What does this say about BAI in this context? That the host clears or tolerates pathogens in each context equally? This is important as it runs against some of the BAI published dogma that bacteria are readily cleared from normal wounds but not from implant-containing wounds.

Authors: The differences between both groups were significant at later time points (at day 16, see Fig. 4). In the present experiments, bacterial clearance was slow in mice without implants. We do not think this necessarily runs against present BAI dogmas, because the rate at which bacteria are cleared clearly depends on the location and the surface characteristics of the implant.

D. Grainger: Is it possible that Xen36 produces some of its bioluminescence that out-survives the bacteria in the tissue site, and leaves an optical emission signature after these bacteria are dead or within the phagocytes? This could explain the 6-day data where both implant and non-implant infections show the same optical signal.

Authors: This is an intriguing question. Bioluminescence is a very sensitive marker for the viability of bacteria. Reduction in the production of ATP and NADPH and availability of oxygen will immediately result in a decrease of bacterial bioluminescence, probably faster than due to the depletion of luciferase. It is well known that bacteria may survive in tissue even within macrophages, but it is unknown however to what extent these bacteria are still able to produce bioluminescence or possibly enhance the production of NADPH counteracting the hostile environment and enhancing bioluminescence radiance.

D. Grainger: Could you include the following information about Xen36? The Xen40 model bioluminescent bacterial product is transformed genetically from the highly reported, virulent osteomyelitis clinical isolate, UAMS-1 (Elrasri *et al*., 2002, additional reference). The Xen36 strain is derived from the bacteraemia clinical isolate ATCC 49525 Pribaz *et al*., 2011, text reference). Additional significant Xen36 infection/luminescent characterisation for this paper is further reported in Bernthal *et al*. (2010) and Bernthal *et al*. (2011) (both additional references).

Authors: Thank you for this comment. We agree that it is useful to add the information concerning virulence and biofilm forming character of the *S. aureus* Xen36 strain.

Additional References

Bernthal NM, Stavrakis AI, Billi F, Cho JS, Kremen TJ, Simon SI, Cheung AL, Finerman GA, Lieberman JR, Adams JS, Miller LS (2010) A mouse model of post-arthroplasty Staphylococcus aureus joint infection to evaluate *in vivo* the efficacy of antimicrobial implant coatings. PloS ONE **5**: e12580.

Bernthal NM, Pribaz JR, Stavrakis AI, Billi F, Cho JS, Ramos RI, Francis KP, Iwakura Y, Miller LS (2011) Protective role of IL-1beta against post-arthroplasty Staphylococcus aureus infection. J Orthop Res **29**: 1621-1626.

Elasri MO, Thomas JR, Skinner RA, Blevins JS, Beenken KE, Nelson CL, Smeltzer MS (2002) S. aureus collagen adhesin contributes to the pathogenesis of osteomyelitis. Bone **30**:275-280.